

PAPER

View Article Online  
View Journal | View Issue



Cite this: *Environ. Sci.: Nano*, 2025, 12, 2034

# Combining *Trichoderma* sp. and biogenic AgNPs from *Trichoderma* strains as a synergistic control complex to improve the growth of muskmelon and suppress *Fusarium oxysporum* f. sp. melonis

Tong Li,<sup>†a</sup> Ran Tao,<sup>†a</sup> Zhen Zhong,<sup>†a</sup> Xian Liu <sup>\*,a</sup> and Zenggui Gao<sup>\*,b</sup>

Muskmelon *Fusarium* wilt (MFW) disease caused by *Fusarium oxysporum* f. sp. *melonis* (FOM) is one of the major challenges faced in muskmelon production worldwide. *Trichoderma* sp., as a well-known biocontrol fungus, and AgNPs have been widely used to control plant diseases. However, few literature studies have been reported on the combined application of AgNPs and *Trichoderma* sp. against soil-borne diseases. This study was aimed at investigating the inhibitory effect of AgNPs and *Trichoderma* sp. to FOM and the control effect of the combined application of AgNPs and *Trichoderma koningiopsis* (TK) against MFW. The characteristics of different AgNPs were also analyzed using various techniques, such as XRD, TEM-EDS, FTIR and TEM. Results showed that TK had the highest inhibition rate (63.77%) against FOM among the four *Trichoderma* strains and had the best resistance to AgNPs, with an average inhibition rate of 5.76% on mycelium growth. Different AgNPs and their combinations had different inhibitory effects on the growth and sporulation of FOM. The inhibition rate of the AgNPs-TH (*T. hamatum*) and AgNPs-TK (*T. koningiopsis*) combination (AgNPs-C) was the highest, reaching up to 50.83%. The specific absorption peaks of AgNPs-TH, AgNPs-TK and AgNPs-C occurred at 420 nm, 323 nm and 320 nm, respectively. XRD and TEM-EDS showed that the crystalline structured nanoparticles were spherical with a diameter ranging from 16.5 nm to 23.4 nm. FTIR results showed that there were more functional group moieties (–OH, –CH<sub>3</sub>, –C–O, etc.) on AgNPs-C, which were involved as a capping and reducing agent in the biosynthesis of AgNPs. The combined application of AgNPs-C and TK decreased the incidence (11.11%) and disease index (2.78) compared with CK-F (77.78% and 48.61, respectively) and improved the growth and plant fresh weight. Thus, the combined application of AgNPs and biocontrol agent (TK) could be used to improve the growth and development of muskmelon and suppress the MFW disease, providing an alternative approach to realize an eco-friendly control of the soil-borne disease.

Received 20th August 2024,  
Accepted 3rd January 2025

DOI: 10.1039/d4en00760c

rsc.li/es-nano

## Environmental significance

*Fusarium* wilt of muskmelon (*Cucumis melo* L.), caused by *Fusarium oxysporum* f. sp. *melonis*, which is a devastating soil-borne pathogen, is considered the most severe infectious disease of this cucurbit. The obstacles related to continuous cropping in the process of muskmelon industrialization and intensive planting (leading to a decline in the quality and yield of muskmelon) are becoming increasingly serious. Meanwhile, the *Fusarium* species produce a range of mycotoxins, mostly trichothecenes and fumonisins, that have a negative impact on the soil ecological environment. These mycotoxins change the nutrient imbalances and microbial diversity in the soil and have the potential to deleteriously affect animal and human health. Therefore, it is necessary to adopt ecological and green prevention and control measures to improve the soil environment and reduce the occurrence of muskmelon *Fusarium* wilt. Owing to their special physical and chemical properties and antifungal activity, nanomaterials will become high-quality alternatives for controlling the muskmelon *Fusarium* wilt in the future. Herein, a synergistic application of AgNPs and a biocontrol agent could be used to reduce the *Fusarium* wilt diseases in muskmelon, which provided an alternative approach to realize an eco-friendly control of this soil-borne disease.

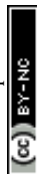
## 1. Introduction

Muskmelon (*Cucumis melo* L.), a key vegetable crop from *Cucurbitaceae*, is rich in fibers, carbohydrates, proteins, vitamins, antioxidants, minerals, and other nutritional elements that are beneficial for people, and it is widely cultivated

<sup>a</sup> College of Bioscience and Technology, Shenyang Agricultural University, Shenyang, 110866, China. E-mail: liuxian7007@syau.edu.cn

<sup>b</sup> College of Plant Protection, Shenyang Agricultural University, Shenyang, 110866, China. E-mail: gaozenggui@syau.edu.cn

<sup>†</sup> Tong Li, Ran Tao and Zhen Zhong contributed equally to this work.



worldwide.<sup>1</sup> Growing populations and the expected higher standard of living will dramatically increase the demand for fresh and high-quality muskmelon in the future in China. As the demand for muskmelon continues to grow, its planting area and multi-cropping index need further increase to improve the muskmelon production in China, which will inevitably lead to the obstacles related to continuous cropping. Muskmelon *Fusarium* wilt (MFW) is caused by the soilborne pathogen *Fusarium oxysporum* f. sp. *melonis* (FOM), a serious disease pathogen that has become prevalent owing to extensive planting of muskmelons.<sup>2,3</sup> This widely distributed disease is considered the most severe infectious disease, with significant impacts on the yield and quality of muskmelon.<sup>4</sup> Some control measures have been used to decrease the incidence of MFW, such as the application of disease-resistant varieties, grafting with other disease-resistant crops, crop rotation, pesticides and strengthening cultivation management. However, these methods are time or labor-intensive, limited by weather and temperature, and pose negative effects on the environment, further leading to a decline in the microbial biomass in the soil.<sup>5</sup> Thus, it is urgent to develop other effective, ecologically compatible and environmental-friendly methods to control MFW.

Biological control is widely recognized as one of the most promising options to manage muskmelon wilt disease.<sup>4,6</sup> Among the beneficial antagonists for plant disease control, *Trichoderma* sp. is widely used as an effective biocontrol agent against various soil-borne pathogens, including the pathogen FOM<sup>7</sup> through a variety of actions, such as competition for space or nutrients, mycoparasitism, antibiosis, inducing resistance, etc.<sup>8,9</sup> Gava *et al.*<sup>8</sup> used *T. harzianum* LCB47, *T. viride* LCB48, *T. koningii* LCB49, and *T. polysporum* LCB50 to control melon wilt in a naturally infested soil. The results showed that the treatment with *T. polysporum* LCB50 (Tp) showed the highest efficiency to control melon wilt (44.85%), increasing the fruit yield to 43%. A strong synergistic effect was observed when applying Tp (seed treatment) and LC25 and LC50 (applying at 15 days after transplanting), resulting in a highly significant wilt control (68% and 72%, respectively) and an increase in productivity. Zhang *et al.*<sup>1</sup> also found that *T. viride* T23 could effectively reduce the disease index of muskmelon wilt at the greenhouse. However, a single biocontrol strain has been proved to show some disadvantages in a generally limited spectrum of target pathogens, decreases in control effect due to adaptability to environmental conditions, and persistence on strain activity.<sup>10</sup> The combined application of biocontrol strains or/with other plant defense elicitors, fertilizers or composts to control soil-borne diseases has been widely used in agriculture practice.<sup>11–14</sup> Furthermore, several studies have focused on the combination of *Trichoderma* sp. with pesticides for controlling crop disease, and higher control effects have been achieved. Zhang *et al.*<sup>15</sup> employed *T. viride* mixed with several pesticides to inhibit the growth of the pathogen responsible for watermelon *Fusarium* wilt, and the *T. viride* combination with 45% prochloraz aqueous emulsion

achieved up to 79.3% inhibition rate. Wang *et al.*<sup>16</sup> investigated the control effect on the synergistic application of *T. harzianum* SH2303 and difenoconazole-propiconazole (DP) against southern corn leaf blight (SCLB). Results showed that the combination of DP and SH2303 reduced the leaf spot area compared to CK, and the efficacy of DP + SH2303 against SCLB could reach up to 15–20 d in the pot trial under greenhouse conditions. The integrated use of *A. indica* leaf extract and bavistin as a seed treatment for chickpea and soil application of *T. harzianum* could decrease the wilt incidence of chickpea, increasing the number of root nodules and chickpea yield.<sup>17</sup> The combined application of *T. asperellum* SC012 with hymexazol could control cowpea wilt disease more effectively than their individual use.<sup>18</sup> The combination of *T. reesei* with mancozeb could inhibit the mycelial growth of *F. oxysporum* F1, which was enhanced by approximately 36% compared to CK in PDA medium.<sup>19</sup> Many literature studies have shown that many *Trichoderma* species, such as *T. asperellum* SC012, *T. harzianum* T-H4, *T. koningiopsis* T-K11, *T. asperellum* T-AS1, *T. hamatum* T-A12, *T. aggressivum* TAET1 and *T. harzianum* Pf 80, were found to be compatible with various fungicides (Vitavax, Topsin, Thiram, Ridomil, Chlorothalonil, Mancozeb, and Captan, etc.),<sup>18,20–22</sup> which provided the basis of the combination of the *Trichoderma* species with fungicides to control soil-borne diseases. The combination of *Trichoderma* sp. and various fungicides could reduce the use of chemical fungicides, which is eco-friendly and may be an important part of the integrated control of *Fusarium* wilt. However, few works have been reported on the synergistic application of silver nanoparticles (AgNPs) and *Trichoderma* sp. against soil-borne diseases, such as MFW.

AgNPs, as one of the important nanomaterials in the nanotechnology industry, are characterized by their distinctive physicochemical properties, including their extremely small size, high specific surface area, good electrical conductivity and strong antimicrobial properties when compared to bulk silver.<sup>23</sup> These properties make them of potential value in the area of agriculture, medicine, electronics and environment.<sup>24</sup> AgNPs have been used to control plant diseases and exhibited strong antifungal activity against various pathogens, including *Aspergillus niger*, *Fusarium* sp. (including fungicide-resistant *F. graminearum* strains), *Candida*, *Raffaelea* sp., *Pythium aphanidermatum*, *Sclerotinia sclerotiorum*, and *Macrophomina phaseolina*.<sup>25–27</sup> The exact mechanism by which AgNPs exert antimicrobial activity remains unclear and is still a debated topic.<sup>28</sup> Some antimicrobial mechanisms of AgNPs have been proposed, including the breakdown of the cell wall and membrane, resulting in the leakage of cellular contents, damaging intracellular structures, causing metabolism dysfunction and organelles destabilization, inactivating the key enzymes and signaling proteins, inducing the production of cellular toxicity and oxidative stress, and modulating the signal transduction pathways, etc.<sup>29–31</sup> Thus, it is challenging for pathogens to develop drug resistance against AgNPs, making them a promising alternative approach to fight antibiotic



resistance and combat against resistant microbes.<sup>25,32</sup> In the agroecosystems, the three major kinds of interactions involving AgNPs focused on soils, microbial populations, and plants. In the soil environment, AgNPs' fate, transport, bioavailability, and toxicity are changed by the soil physicochemical properties, including soil texture, pH, cation exchange capacity, and soil organic matter.<sup>33</sup> Although AgNPs are gradually being recognized as a promising alternative to conventional fungicides in controlling plant disease, their impact on soil biota is still being studied and has attracted more attention. Previous studies have shown that dose-dependent silver nanoparticles have different effects on soil biodiversity, population structure, and microbial processes. The impact of AgNPs on soil microbial community was also dependent on soil types, along with environmental parameters.<sup>34,35</sup> Low concentrations of AgNPs into the soil may be favorable for microbial processes with no hindrance in beneficial plant-microbe interactions in agroecosystems. Earlier reports focusing on the impact of AgNPs on plants have yielded both positive and negative effects. The phytotoxicity of AgNPs is basically controlled by plants (seeds, species type, growth stage), AgNPs (size, concentration, mode of application), and experimental conditions (time and method of AgNP exposure). Due to the scarcity of literature studies on the application of biosynthesized AgNPs in agriculture, the impact of biologically synthesized AgNPs on soil microbiota and plants remains unclear. Therefore, when talking about the application of AgNPs in agroecosystems, their major interactions with the residing soil and various biota need to be further studied.<sup>36</sup> Thus, a study on the combination effect of biosynthesized AgNPs and *Trichoderma* sp. on the control of MFW is helpful to evaluate the effect of AgNPs on the soil microbials and plants.

This study aimed to systematically investigate the antifungal activity of AgNPs and *Trichoderma* sp. against the FOM and screen *Trichoderma* sp. with resistance to AgNPs. Then, pot experiments were conducted to study the combination of AgNPs with the AgNPs-resistant *Trichoderma* strain to control the muskmelon *Fusarium* wilt, and improve the growth and development of muskmelon. The idea of this study is to give full play to the rapid and direct fungicidal action of AgNPs and the rapid growth of *Trichoderma* strain, occupying ecological niche and promoting its growth on muskmelon to improve the control effect for MFW. This study will advance the understanding of AgNPs + *Trichoderma* sp. applications for plant disease control, with the main goal of decreasing the incidence of muskmelon *Fusarium* wilt, enhancing the plant health, and reducing the pathogen resistance.

## 2. Materials and methods

### 2.1 Microorganisms and reagents

*T. atroviride*-XML (TA-XML), *T. atroviride*-FC (TA-FC), *T. koningiopsis* (TK), *T. hamatum* (TH) were originally isolated from the roots of oak trees, and the spores were maintained at 4 °C

on silica gel pellets at the culture collection of the Sericulture lab, Shenyang Agricultural University, China. Then, it was re-cultivated before use in silver nanoparticles biosynthesis and biocontrol on MFW.

*Fusarium oxysporum* was originally isolated from muskmelon root with the typical symptoms of muskmelon *Fusarium* wilt disease, and was kept at 4 °C in the Sericulture lab.<sup>37</sup>

Muskmelon (*Cucumis melo* L.) seeds (Jingtiang no. 1) were purchased from Yue Nong seedling Co., LTD (Shenyang, China).

AgNO<sub>3</sub> (AR Grade) was purchased from Sinopharm Chemical Reagent Co., Ltd (Shanghai, China).

### 2.2 AgNP biosynthesis

Biosynthesis of AgNPs was performed, as described by Cui *et al.*<sup>38</sup> The cell-free supernatant of different *Trichoderma* strains was prepared by culturing fungus in potato dextrose broth (PDB) contained (g L<sup>-1</sup>): 200.0, fresh potato cubes, and 20.0, dextrose, at 28 °C and 100 rpm for 72 h, then filtering with Whatman filter paper no. 1. Cell-free supernatants (100 mL) were mixed with silver nitrate solution (final concentration: 2.0 mmol L<sup>-1</sup>; adjusting pH to 7 with nitric acid) and incubated at 55 °C for 24 h under light conditions. The resultant AgNPs reaction solutions were tested by UV-visible spectrometry in the wavelength range of 300–800 nm. AgNPs in the reaction solution was collected by centrifugation at 10 000 g for 30 min, washed twice with sterile distilled water and with 75% ethanol once, then stored at -20 °C.

### 2.3 Dual culture test

The antagonistic effect of *Trichoderma* isolates against FOM were evaluated by adopting the confrontation assay of Sánchez-Montesinos *et al.*<sup>22</sup> Petri dishes (9 cm diameter) containing about 17 mL of PDA (g L<sup>-1</sup>: 200.0, fresh potato cubes; and 20.0, dextrose and 20, agar) were prepared. Then, 1 cm plugs of mycelium cut from the fringe of 5 days grown fungal colony were placed at the ends of Petri dishes with a distance of 6.0 cm between *Trichoderma* sp. and FOM, in triplicate. Controls were prepared by only transferring the FOM plug on the plate. All plates were sealed with Parafilm and incubated in the dark at 25 °C for 4 days. Radial fungal colony growth was measured to calculate the inhibition rate of *Trichoderma* sp. to FOM.

### 2.4 Antifungal activity of biosynthesized AgNPs

The antifungal activity of AgNPs was assayed by controlling the mycelial growth and sporulation of FOM and *Trichoderma* sp. The mycelium plugs ( $d = 1$  cm) from the fringe of a fungal colony grown for 4–7 days was transferred to the middle of a PDA medium containing AgNPs (100 mg L<sup>-1</sup>), in triplicate. Controls were prepared using potato dextrose agar only. Then, plates were incubated for 4 days for *Trichoderma* sp. and 7 days for FOM at 25 °C, and the diameter of the colonies were measured to calculate the inhibition ratio of



AgNPs to the two fungi. At the 15th day, the spore amounts of the two fungi were determined with a hemocytometer.

## 2.5 Characterization of synthesized AgNPs

The spectra of the three AgNPs (AgNPs-TK, AgNPs-TH and their combination AgNPs-C) were measured in the wavelength range of 300–800 nm, with a resolution of 1 nm using a UV/vis spectrophotometer (UV-vis U-3010, Japan). The X-ray diffraction pattern of AgNPs was analyzed by a diffractometer (BRUKER D8-Advance, Germany) operating with Cu  $K\alpha_1$  radiation generated at an accelerating voltage of 40 kV and 30 mA with a scan rate of  $3^\circ \text{ min}^{-1}$  for  $2\theta$  values between  $30\text{--}85^\circ$ . The AgNPs shape and size were obtained from a transmission electron microscope (JEOL JEM-2100F/Talos F200x, Japan) operating at 40 kV, where a drop of aqueous AgNPs was loaded on a carbon-coated copper grid, and allowed to dry at room temperature. Elemental analysis of the biosynthesized AgNPs was studied using TEM (JEOL JEM-2100F/Talos F200x, Japan) operated at 40 kV, and coupled with energy dispersive analysis for compositional analysis and the presence of elemental silver.<sup>39</sup> The FTIR spectrum was measured using a spectrometer (Nicolet IS50, USA) in the wavelength range of  $400\text{--}4000 \text{ cm}^{-1}$  at a resolution of  $4 \text{ cm}^{-1}$  to analyze the functional groups using the powder of AgNPs in KBr pellets.

## 2.6 Pot experiment

Full muskmelon seeds were surface-sterilized with 10% sodium hypochlorite for 10 min, and further treated with warm water at  $50^\circ \text{C}$  for 2 h. The seeds were wrapped into wet sterile gauze, then put into an incubator at  $30^\circ \text{C}$  for germination. The treated seeds were sown in plastic pots filled with about 250 g nutrient matrix. After 30 days of cultivation at  $26^\circ \text{C}$ , 50 mL of AgNPs-C solution ( $100 \text{ mg L}^{-1}$ ),  $1 \times 10^6 \text{ CFU mL}^{-1}$  TK spore suspension, and their combination were watered into a pot, representing AgNPs-C, TK and AgNPs + TK treatment, respectively. The control (including CK-W and CK-F) were watered with 50 mL sterile water. There were 6 pots at every treatment, in triplicate. Continuing the culturing for 5 days, the muskmelon seedling roots were slightly injured by cutting the soil around the melon roots at a cross shape with a knife, and 30 mL of FOM spore suspension ( $1 \times 10^6 \text{ CFU mL}^{-1}$ ) was inoculated into the pots for the CK-F, AgNPs, TK and AgNPs + TK treatments. At CK-W treatments, pots were watered with 30 mL sterile water only. 20 days after inoculation, the incidence and disease index were calculated basing on the wilt status and root infestation of the plant. At the same time, the plant root and stem length, and the fresh weight of the above-ground portion and roots were measured to evaluate the development and growth of the muskmelon seedlings.

## 2.7 Statistical analyses

Statistical analyses were conducted using SPSS for Windows, Version 22.0 and Graphpad Prism 6.0 (GraphPad, San Diego, USA). All the experimental data were presented as the mean  $\pm$

standard deviation (SD). One-way analysis of variance (ANOVA) was conducted to compare the differences of the means. Dunnett's test was performed for multiple comparisons, and the Student's *t*-test was performed for each dataset, comparing with the control data. The statistical significance for all tests was considered at a probability level of 0.05 ( $P < 0.05$ ) or 0.01 ( $P < 0.01$ ).

# 3. Results

## 3.1 Screening of *Trichoderma* strains with high inhibitory effect on FOM

The inhibitory effect of different *Trichoderma* strains on FOM was studied using the confrontation culture (Fig. 1). The results showed that different *Trichoderma* strains had different inhibitory effects on FOM. Among them, *T. koningiopsis* had the highest inhibitory rate against FOM, reaching up to 63.77%, while *T. hamatum* had the lowest inhibitory rate against FOM, at only 39.56% (Fig. 1A). At the same time, it was also found that different *Trichoderma* strains had different antifungal modes on FOM. *Trichoderma koningiopsis* could grow and cover the mycelium of FOM, showing a mycoparasitic effect on FOM. Conversely, *T. atroviride*-FC and *T. hamatum* could not grow on the mycelium of FOM (Fig. 1B). For a more comprehensive analysis, *T. koningiopsis* was screened as the best biocontrol agent to further study its control effect on MFW in the pot experiment.

## 3.2 The inhibitory effect of different AgNPs and their combination from different *Trichoderma* sp. on FOM

The antifungal activities of AgNPs on FOM were determined by the mycelium growth rate method. After 7 d of culture, the colony diameter and spore production of FOM were measured to analyze the inhibitory effect of AgNPs on FOM (Fig. 2). The results showed that different AgNPs and their combination had different inhibitory effects on the growth and sporulation of FOM. In the single AgNPs treatments, AgNPs-TK had the highest inhibitory rate on FOM, reaching 38.98%, while AgNPs-TA-FC had the lowest inhibitory rate on FOM, at only 22.53%. In the AgNPs combination treatments, the inhibition rate of AgNPs-TH and AgNPs-TK combination was the highest, reaching 50.83% (Fig. 2A).

Different AgNPs and their combinations caused inhibition in the sporulation of FOM (Fig. 2B). There were not significant differences among different AgNPs treatments, and better sporulation inhibition was found at AgNPs-TK and the combination of AgNPs-TH and AgNPs-TK. Compared with CK ( $3.15 \times 10^7 \text{ CFU mL}^{-1}$ ), AgNPs could make the spore amounts decrease by about one/two orders of magnitude. The spore amounts of AgNPs-TK and the combination of AgNPs-TH and AgNPs-TK only reached up to  $4.67 \times 10^5$  and  $6.67 \times 10^5 \text{ CFU mL}^{-1}$ , respectively. Comprehensive analysis of the results of silver nanoparticles on the mycelium growth and sporulation of FOM showed that the combination of AgNPs-TH and AgNPs-TK had a better inhibitory effect on FOM (Fig. 2C).



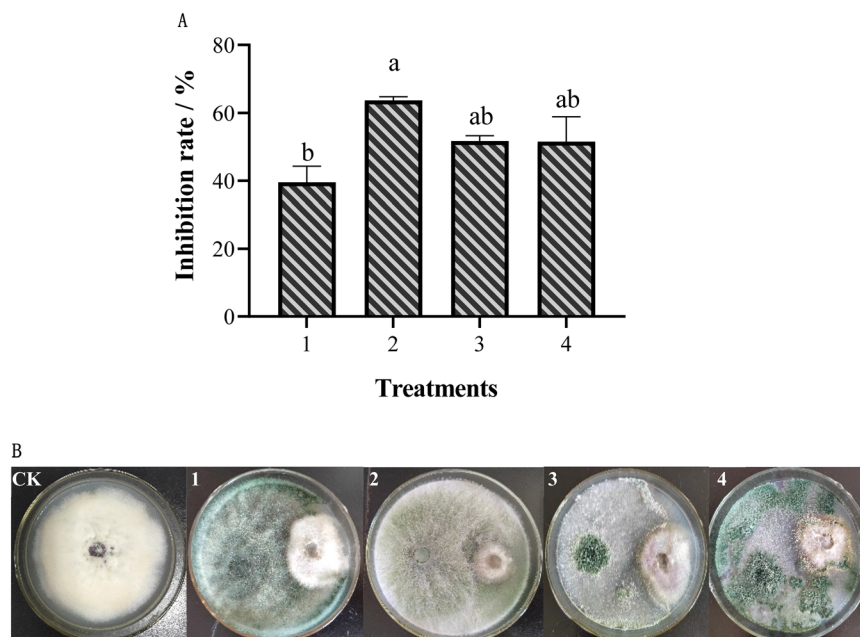


**Fig. 1** Inhibition effect of different *Trichoderma* strains on *Fusarium oxysporum*. (A) Inhibition rate; (B) colony morphology of dual confrontation; 1: TH; 2: TK; 3: TA-FC; 4: TA-XML. Different letter(s) in the same column differ significantly according to Duncan's test ( $p < 0.05$ ).

### 3.3 The *Trichoderma* strains resistance to the AgNPs

It was revealed from study that different *Trichoderma* strains showed different resistances to different AgNPs by measuring the mycelium growth and sporulation of *Trichoderma* strains on the PDA medium containing AgNPs (Fig. 3). The growth of *T. koningiopsis*, in terms of the colony diameter, was slightly inhibited (Average inhibition rate was 5.76%) on day 3 by AgNPs, whereas the growth of the other three *Trichoderma* strains was greatly inhibited (Average inhibition rate were 56.63% (*T. hamatum*), 57.98% (*T. atroviride*-XML) and 60.25% (*T. atroviride*-FC), respectively) (Fig. 3A). Spore production also showed that *T. koningiopsis* had the highest resistance to AgNPs, which was the same for the mycelium growth (Fig. 3B). According to these results, *T. koningiopsis* was screened to further study its resistance to the different AgNPs combinations. Some AgNPs combinations had higher inhibitory effect on the mycelium growth, but showed a stimulation effect on sporulation (Fig. 3C and D). The combination of AgNPs-TH and AgNPs-TK had the lower inhibition ratio on TK, and did not affect the sporulation of TK. Our data clearly demonstrated that different *Trichoderma* strains had different resistance to different AgNPs, according to the mycelium growth and spore production (Fig. 3E).

Based on the comprehensive analysis of the inhibitory effects of different AgNPs and their combinations and different *Trichoderma* strains on FOM, and the resistance of different *Trichoderma* strains to AgNPs and their combinations, the combination of AgNPs-TH and AgNPs-TK (AgNPs-C) and *T. koningiopsis* were screened for further study of their synergistic control effect on MFV.

### 3.4 Characterization of synthesized AgNPs

The *Trichoderma* strains culture liquid was mixed with  $\text{AgNO}_3$  for 24 h to biosynthesize the AgNPs. During the process of AgNPs production, the color of the reaction mixture turned from light yellow to dark brown, indicating  $\text{AgNO}_3$  reduction to AgNPs. The specific absorption peak of AgNPs-TH, AgNPs-TK and AgNPs-C occurred at 420 nm, 323 nm and 320 nm, respectively (Fig. 4), which further confirmed the biosynthesis of AgNPs and presence of silver element (Cui *et al.*, 2022). Then, three AgNPs samples were subjected to XRD, TEM-EDS, FTIR and TEM analysis. The XRD pattern of AgNPs is shown in Fig. 5. The diffraction peaks at  $2\theta = 38.12^\circ$ ,  $44.28^\circ$ ,  $64.47^\circ$  and  $77.47^\circ$  were assigned to the corresponding lattice plane values of (111), (200), (220) and (311), respectively, which indicated the cubic crystal structure of three kinds of AgNPs (JCPDS no. 04-0783).

To further validate the presence of the Ag element, AgNPs samples were analyzed via TEM-EDS (Fig. 6). The EDS spectrum showed a strong peak at approximately 3 keV, which is typical for the absorption of silver crystallites according to surface plasmon resonance. In addition, there were some other weak peaks probably from copper, carbon and other elements for the copper grid or culture medium, which are also shown in the TEM graph (Fig. 6).

FTIR was used to identify the functional groups involved in the coating of AgNPs. Infrared absorption spectra were obtained for the samples, reflecting the characteristics of the chemical bonds present. The FTIR analysis of the three kinds of AgNPs showed intense peaks at  $3435.69\text{ cm}^{-1}$ ,  $1627.23\text{ cm}^{-1}$ ,  $1019.49\text{ cm}^{-1}$  and  $569.76\text{ cm}^{-1}$  in AgNPs-TK;  $3440.80\text{ cm}^{-1}$ ,  $1628.74\text{ cm}^{-1}$ ,  $1024.62\text{ cm}^{-1}$  and  $571.55\text{ cm}^{-1}$  in AgNPs-TH; and  $3431.44$



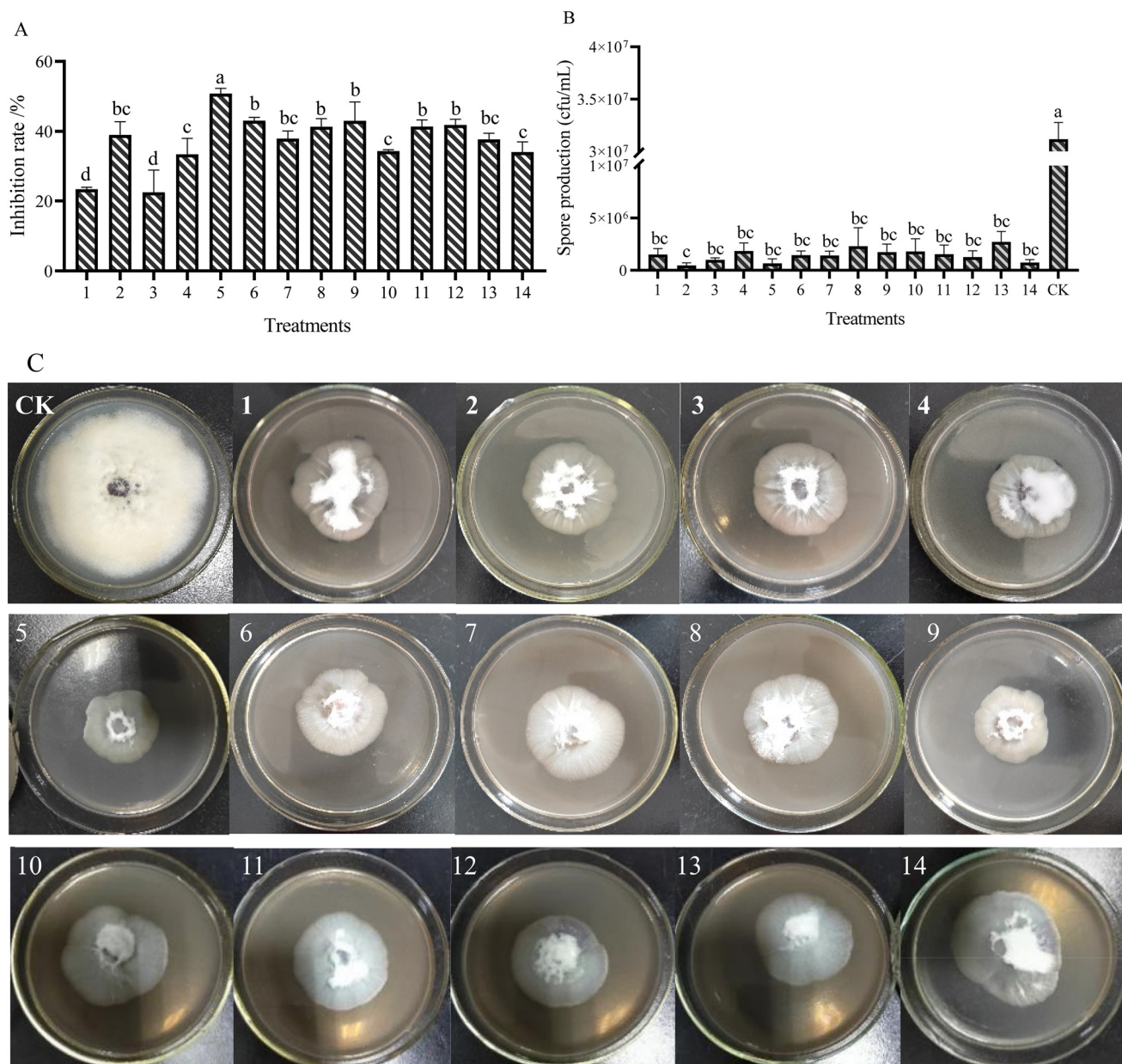


**Fig. 2** AgNPs impair the growth and asexual development of *F. oxysporum*. (A) Inhibition rate of mycelium growth. (B) Spore production inhibited by AgNPs. (C) Colony morphology of the FOM cultured on PDA containing different AgNPs for 7 days. 1–14 present the different AgNPs and their combination. 1: AgNPs-TH; 2: AgNPs-TK; 3: AgNPs-TA-FC; 4: AgNPs-TA-XML; 5: 1 + 2; 6: 1 + 3; 7: 1 + 4; 8: 2 + 3; 9: 2 + 4; 10: 3 + 4; 11: 1 + 2 + 3; 12: 1 + 2 + 4; 13: 2 + 3 + 4; 14: 1 + 2 + 3 + 4. Different letter(s) in the same column differ significantly according to Duncan's test ( $p < 0.05$ ).

$\text{cm}^{-1}$ ,  $1632.98 \text{ cm}^{-1}$ ,  $1384.51 \text{ cm}^{-1}$ ,  $1026.56 \text{ cm}^{-1}$  and  $573.28 \text{ cm}^{-1}$  in AgNPs-C (Fig. 7). These peaks correspond to some functional groups, such as the  $-\text{OH}$  group of phenols,  $\text{C}=\text{C}$  stretching modes of the vibration in alkyne groups,  $-\text{C}-\text{O}$  stretch of alcohols, carboxylic acids and esters, etc. There were different functional groups among the three kinds of AgNPs, and more functional groups in AgNPs-C.

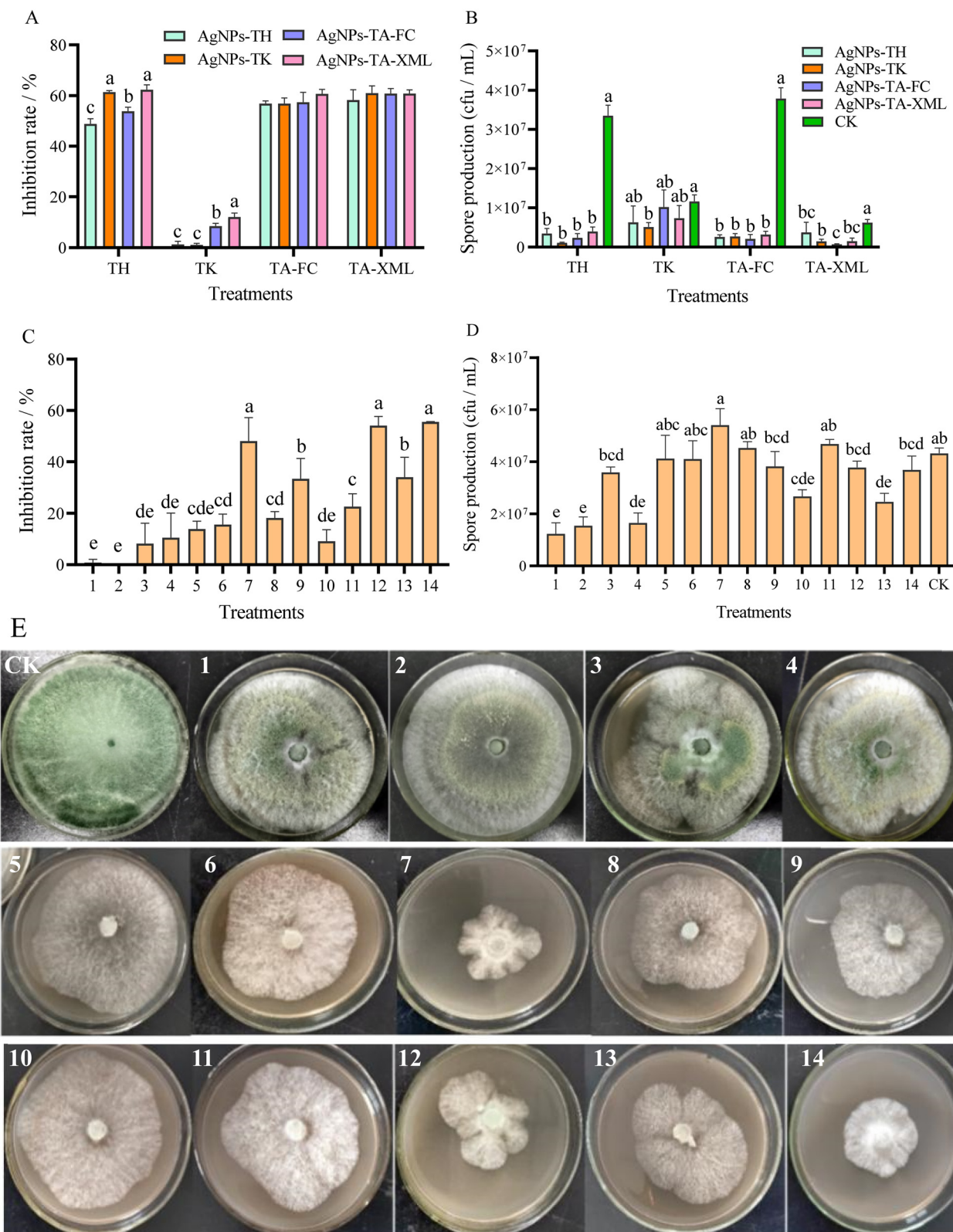
The TEM images showed that the nanoparticles were spherical in shape and well dispersed (Fig. 8). A white layer around the nanoparticles as the coating might prevent nanoparticle agglomeration. In addition, AgNPs showed a crystalline structure with the size distribution of the majority

of NPs ranging from 20.80 nm to 23 nm (AgNPs-TK), 21.30–23.40 nm (AgNPs-TH) and 16.50–19.00 nm (AgNPs-C).

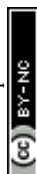
### 3.5 Synergetic control of *T. koningiopsis* with AgNPs to MFW

Symptoms of *Fusarium* wilt appeared on day 20 after the muskmelon seedlings were inoculated with the spore suspension of FOM. The disease incidence and disease index were then assessed according to the disease grade. The results showed that there were extremely significant differences among the treatments for disease incidence and disease index (Fig. 9). There were no diseased plants for the





**Fig. 3** AgNPs impair the growth and asexual development of *Trichoderma* sp. (A) Inhibition rate of mycelium growth. (B) Spore production inhibited by AgNPs. (C) Inhibition rate of different AgNPs and their combination on the growth of TK. (D) TK spore amount under different AgNPs and their combination. (E) Colony morphology of TK cultured on PDA containing different AgNPs for 7 days. 1–14 present the different AgNPs and their combination. 1: AgNPs-TH; 2: AgNPs-TK; 3: AgNPs-TA-FC; 4: AgNPs-TA-XML; 5: 1 + 2; 6: 1 + 3; 7: 1 + 4; 8: 2 + 3; 9: 2 + 4; 10: 3 + 4; 11: 1 + 2 + 3; 12: 1 + 2 + 4; 13: 2 + 3 + 4; 14: 1 + 2 + 3 + 4. Different letter(s) in the same column differ significantly according to Duncan's test ( $p < 0.05$ ).



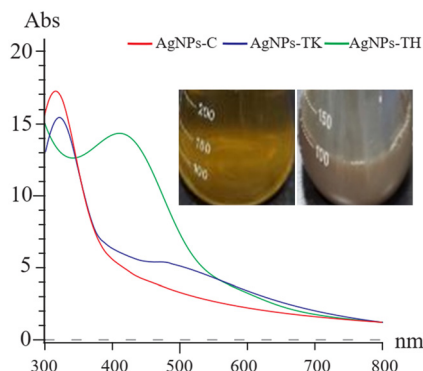


Fig. 4 UV-vis spectra of three AgNPs. The inset shows the color change of the reaction solution.

CK-W, and the disease incidence in the AgNPs, TK and AgNPs + TK treatment was less than 28%, which was significantly lower than that in the CK-F treatments (77.78%). Pot experiments showed that AgNPs, TK or TK + AgNPs-C treatment could reduce disease incidence, in which the AgNPs + TK treatment was the best (only 11.11%). The manifestation of the disease index was basically consistent with the disease incidence. The disease index for the AgNPs + TK treatment was the lowest (only to 2.78), which showed that AgNPs + TK could decrease the disease severity.

### 3.6 Synergetic effect of *T. koningiopsis* with AgNPs on the growth and development of muskmelon

The interactive effects of the *Trichoderma* strain and AgNPs were significant for plant growth traits, like the root and stem length, fresh weight of above-ground plant portion and roots. One-way ANOVA exhibited significance for the root length and stem, and the fresh weight of the root and above-ground portion was at  $p \leq 0.05$  levels (Fig. 10). Overall, the AgNPs + TK treatment performed better for plant growth and weight among the disease-control treatments. The root length and stem length for the AgNPs + TK treatment reached up to 34.11 cm and 23.54 cm, respectively, which were very close to that for CK-W (35.41 cm and 26.88 cm) (Fig. 10A and B). The root fresh weight for the AgNPs + TK treatment was 0.18 g per plant, which was greater than that of CK-W (0.15 g per plant) (Fig. 10C). Similar to the growth, the fresh weight of the above-ground portion with AgNPs + TK treatment was 1.89 g per plant, which was similar to that for CK-W (2.06 g per plant) (Fig. 10D). Our data showed that AgNPs, *Trichoderma* strain and their combination could improve the growth and development of muskmelon, further enhancing the plant resistance to the *Fusarium* wilt of muskmelon.

## 4. Discussion

Muskmelon *Fusarium* wilt is the most severe infectious disease, impacting the muskmelon production in both greenhouse nurseries and on the fields. At present, there is still no simple, green and efficient option to control MFW because its pathogen FOM survives in the soil for a long time as chlamydospores.<sup>4</sup>

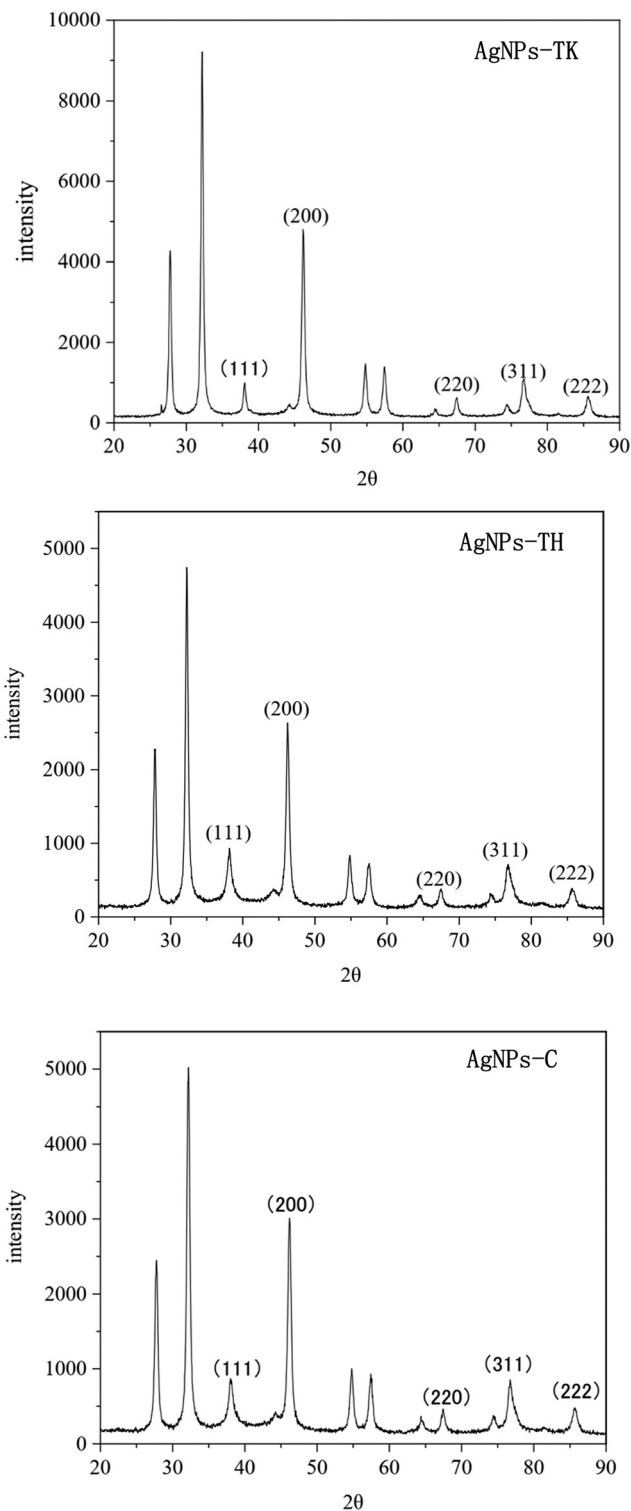
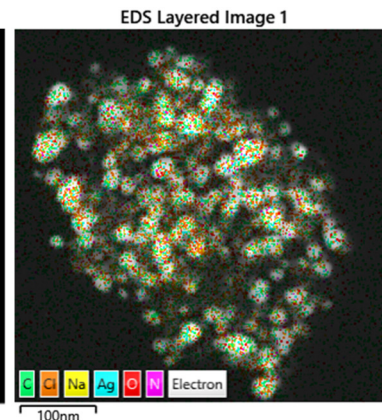
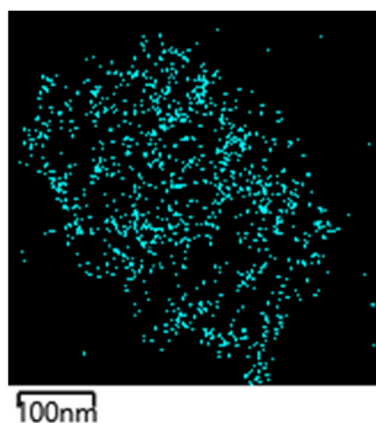
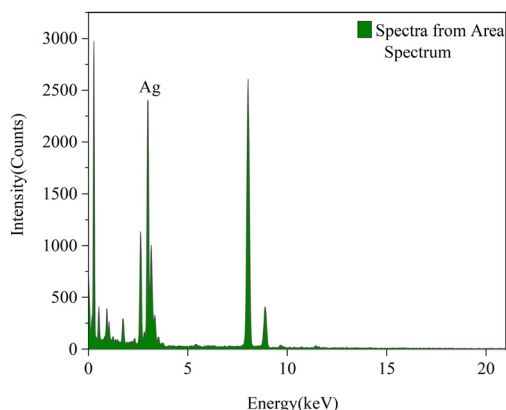


Fig. 5 XRD diffractograms of three kinds of AgNPs.

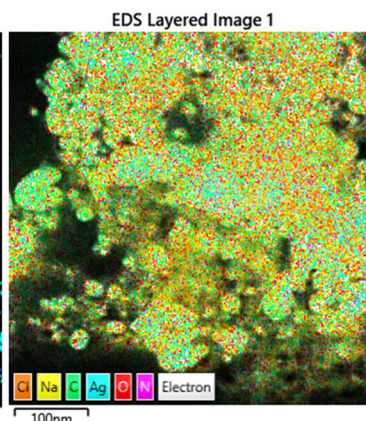
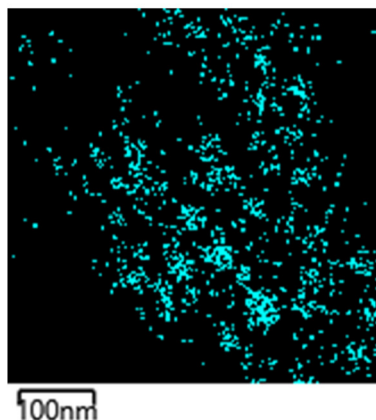
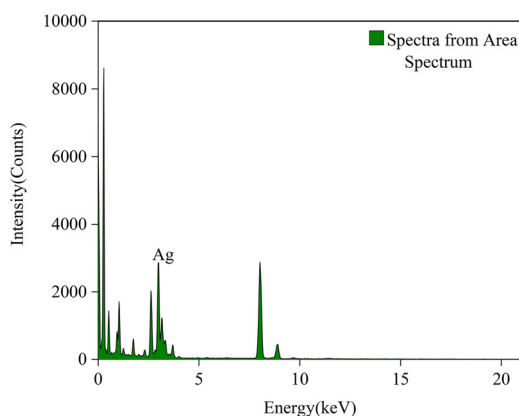
Hence, it is urgent to explore alternative fungicides, biocontrol agents and plant protection strategies toward controlling the MFW in the future. AgNPs, as a broad-spectrum active agent, have been widely used against various phytopathogens, such as *Fusarium* sp., *Phytophthora ultimum*, *Magnaporthe grisea*, *Scalierotinia sclerotiorum* and *Rhizoctonia solani*.<sup>40</sup> In this study, we observed



## AgNPs-TK



## AgNPs-TH



## AgNPs-C

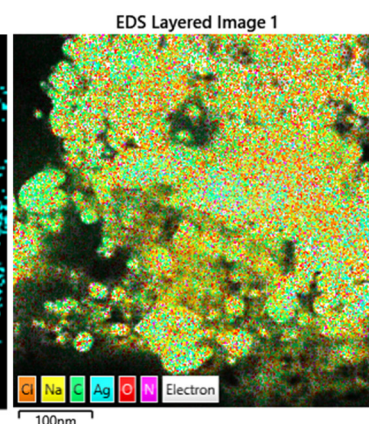
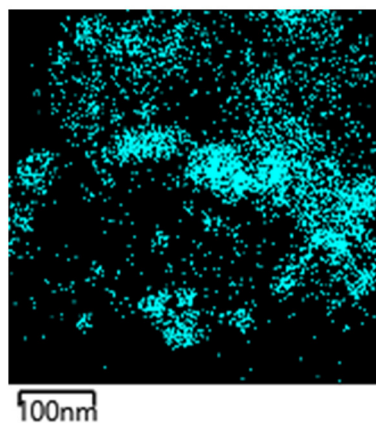
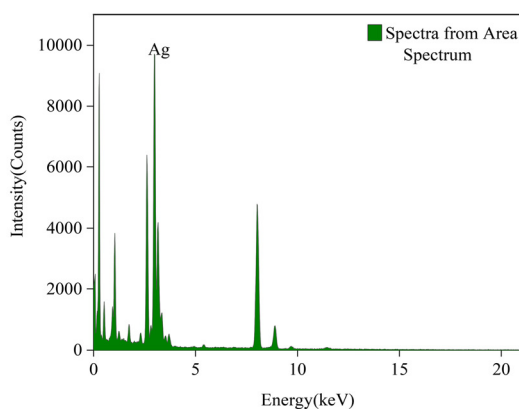


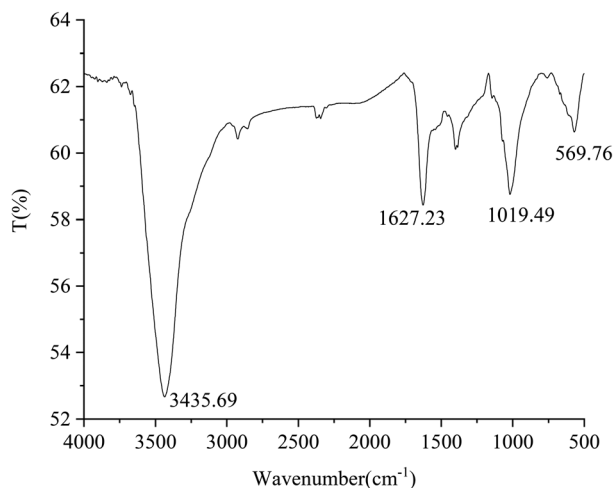
Fig. 6 EDS spectra of three kinds of AgNPs (left), and distribution of silver (middle) and other elements in elemental mapping (right).

that the different AgNPs biosynthesized with different *Trichoderma* strains and these AgNPs combinations showed different inhibitory effects on the growth and sporulation of FOM. The combination of AgNPs-TK and AgNPs-TH (AgNPs-C) had the highest inhibition rate, reaching up to 50.83%. Li *et al.*<sup>41</sup> also found that AgNPs of different sizes (5 nm, 15 nm and 55 nm) had different antibacterial activity, in which AgNPs

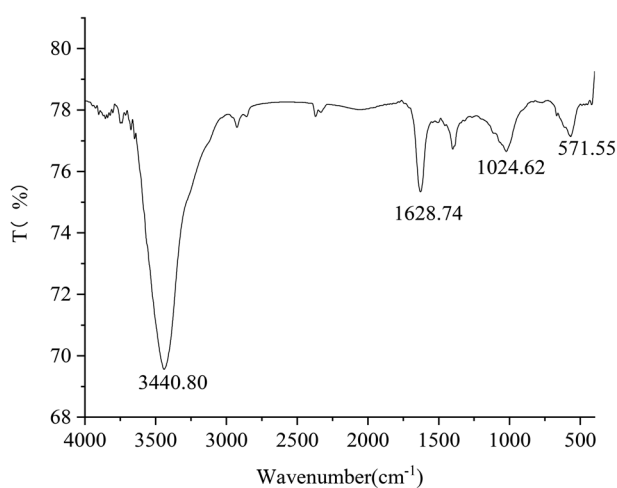
that were 5 nm in size presented the highest antibacterial activity against both Gram-negative and Gram-positive bacteria. In the review paper by Wahab *et al.*, AgNPs with sizes ranging from 5 nm to 57 nm showed strong antimicrobial activity,<sup>29</sup> which were in agreement with our study that the AgNPs exhibiting high antifungal activity were in the size range of 16.50–19.00 nm. Different shapes of AgNPs showed their



## AgNPs-TK



## AgNPs-TH



## AgNPs-C

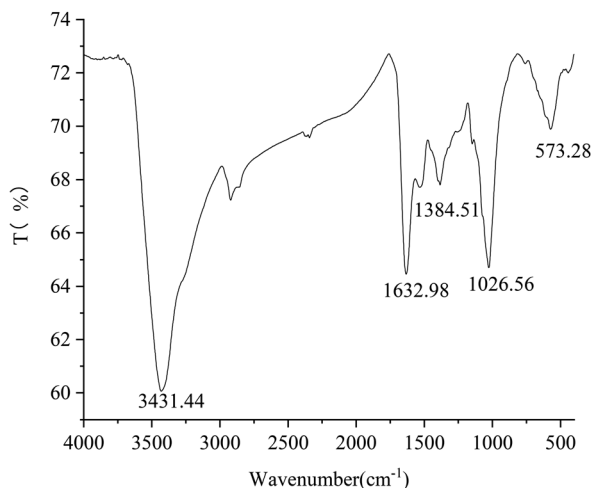


Fig. 7 Fourier-transform infrared absorption spectra of three kinds of AgNPs.

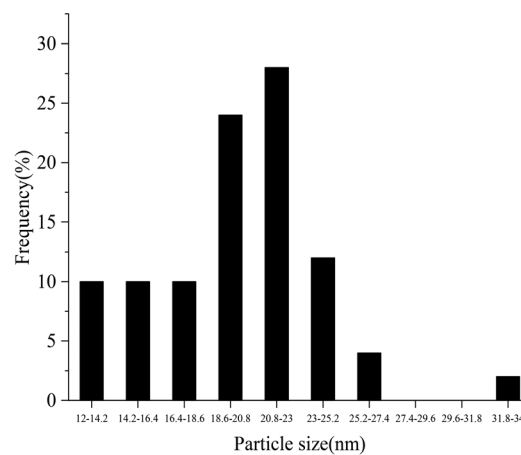
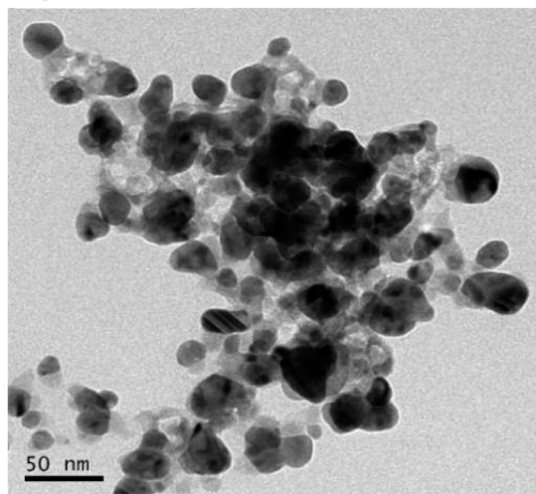
different antimicrobial activity by damaging the membrane. The spherical shape AgNPs biosynthesized from plants and microbes showed significant antimicrobial activity against various pathogens.<sup>42–44</sup> In our study, AgNPs from *Trichoderma* sp. were spherical and face-centered cubic in shape. Furthermore, functional groups involved in the coating of AgNPs may contribute to their antifungal activity.<sup>45</sup> These functional groups, such as  $-\text{COOH}$ ,  $-\text{OH}$ , or  $-\text{C}=\text{O}$  etc., resulted in greatly increased negative charge on the AgNPs surface, which changed the zeta potential of AgNPs to affect the antimicrobial activity.<sup>29</sup> Our study results also displayed more functional groups in AgNPs-C with high antifungal activity, which indicated that these additional functional groups favored increasing antifungal activity.

The approach of biosynthesized silver nanoparticles as fungicides for the control of agricultural pathogens is an innovative pathogen control strategy,<sup>46</sup> because it can make full use of the advantages of AgNPs as a rapid sterilization material that minimizes pathogen resistance. As mentioned in the introduction, AgNPs show many different modes to kill/inhibit microorganisms and achieve the low resistance development.<sup>47</sup> Shi *et al.*<sup>30</sup> observed the hyphae change, spore germination and appressorium formation of *Magnaporthe oryzae* with a light microscope, SEM and TEM after 2 hours treated with AgNPs. The hyphae were collapsed and aberrant after treatment with AgNPs, and there were fissures on the fungal cell wall. The conidial germination and appressorium formation were suppressed by  $2 \mu\text{g mL}^{-1}$  AgNPs. These results suggested that the inhibition of mycelial growth may be associated with the cell wall damage caused by AgNPs. Liu *et al.*<sup>31</sup> also found that AgNPs biosynthesized with *Trichoderma longibrachiatum* could lead to defects in the cell wall of *Fusarium oxysporum*, and the accumulation of vacuoles or vesicles in the cytoplasm after 24 hours treatment. The contents of proteins and carbohydrates in the culture medium were higher than those in the cell at the AgNPs-treated mycelium. The MDA content in the mycelium treated with AgNPs was significantly higher than that without AgNPs treatments. Protective enzymes, such as catalase (CAT), superoxide dismutase (SOD), and peroxidase (POD), in the mycelium increased firstly, then decreased with AgNPs treatment, thereby affecting the removal of reactive oxygen species. These results showed that AgNPs could quickly affect the physiological and biochemical changes of the fungus, and cause the death of mycelium cells. Many literature studies have also shown that AgNPs can inhibit the germination of spores and the growth of the fungus mycelium in a short time.<sup>25,48</sup>

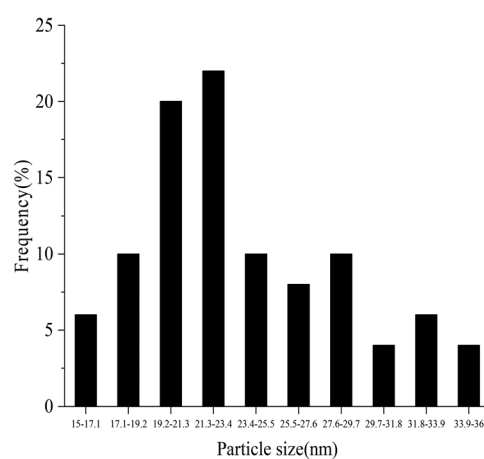
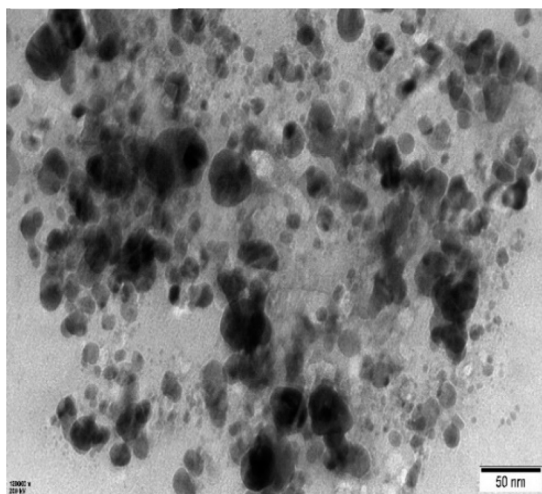
*Trichoderma* sp., as a well-studied biocontrol agent against various plant pathogens, has the ability to suppress plant diseases.<sup>49,50</sup> As an important biocontrol agent, *Trichoderma* sp. performs various biocontrol actions, including competitive role, mycoparasitism, antibiosis effect, induced systemic resistance and antagonism to inhibit or kill pathogens.<sup>51</sup> *Trichoderma* sp. has fast mycelial growth and strong adaptability to the environment.<sup>52–54</sup> It can soon colonize the roots of plants to hinder the invasion of pathogens, and rapidly absorb the nutrients to inhibit the growth and reproduction of the



## AgNPs-TK



## AgNPs-TH



## AgNPs-C

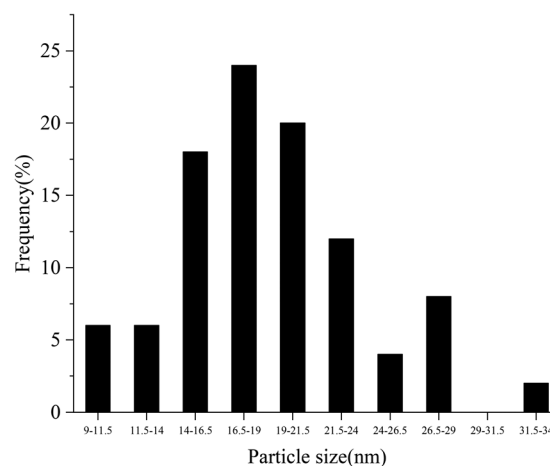
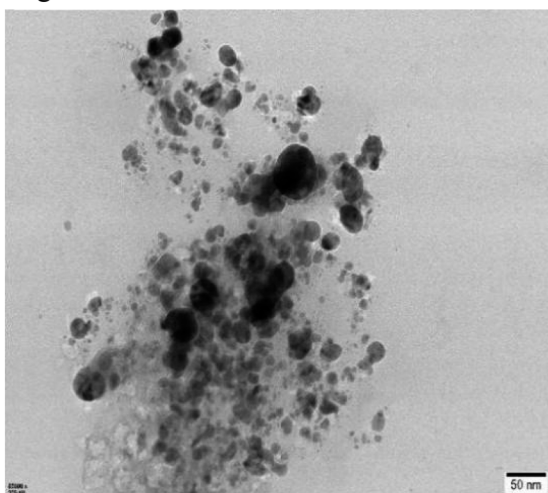
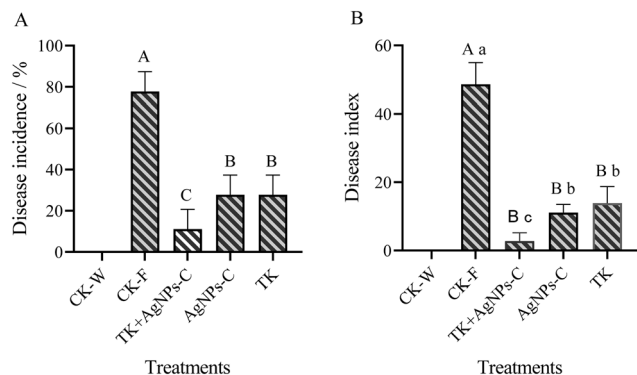


Fig. 8 Transmission electron micrographs of AgNPs (left) and particle diameter distribution of AgNPs (right).





**Fig. 9** Integrative control of TK + AgNPs on the MFW. (A) Disease incidence of MFW. (B) Disease index of MFW. Values in the same column, followed by different lowercase and uppercase letters, are significantly different at the 0.05 and at 0.01 levels, respectively.

pathogens. The present works demonstrated that *T. koningiopsis* showed a strong inhibitory effect and mycoparasitic effect on FOM, and pot experiments indicated the potential of the *Trichoderma* isolate *T. koningiopsis* to reduce muskmelon wilt

caused by FOM and improve muskmelon growth. The results from the dual culture and pot experiments provided solid evidence that TK is a potential biocontrol agent against FOM. Certainly, similar to other biocontrol agents, *Trichoderma* isolates face many challenges in terms of instability and persistence in biocontrol efficiency due to various stresses from the environmental changes and different plant pathogens.<sup>55</sup> Now, many literature studies have confirmed that the integrated control strategies through the combination of *Trichoderma* with fungicides or compost should be developed to improve the sustainability of disease control and to reduce the use of chemical fungicides. Jangir *et al.*<sup>56</sup> used the biocontrol agent (*T. harzianum* MTCC3928) formulated with oilseed cake (OSC) to control *F. oxysporum* f. sp. *lycopersici* infected vascular wilt in *Solanum lycopersicum*, and found that the combination of the biocontrol agent and mustard cake showed 48% disease reduction, and ~40% with *T. harzianum* alone in comparison to the untreated control, and significantly enhanced the growth of *S. lycopersicum*. Ruano-Rosa *et al.*<sup>57</sup> observed that the combined use of *T. atroviride* or *virens* with fluazinam at 0.01 mg L<sup>-1</sup> showed greater *in vitro* growth inhibition of *R. necatrix* (36%

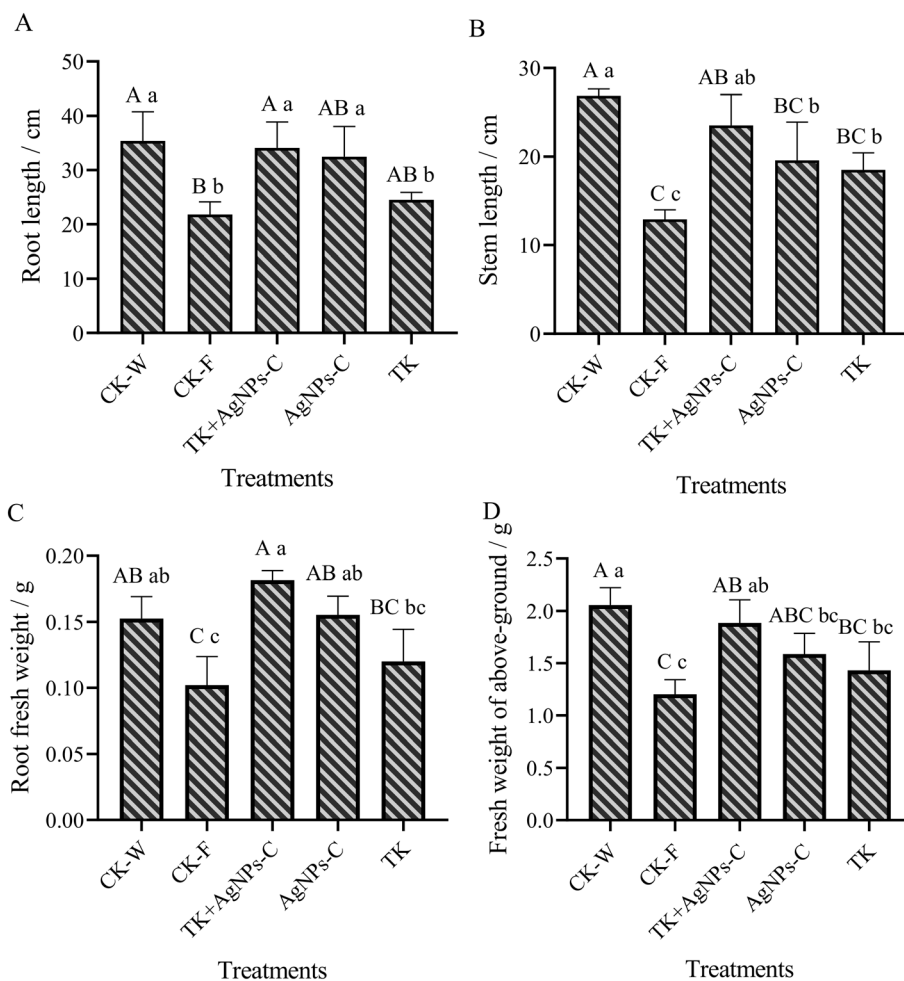


**Fig. 10** Effect of AgNPs, *T. koningiopsis* and their combination on the physiological indicators of muskmelon. Values in the same column followed by different lowercase and uppercase letters are significantly different at the 0.05 and at 0.01 levels, respectively.



and 65%, respectively) than the use of fluazinam alone (23%). Furthermore, the combination of fluazinam at 0.001% with *Trichoderma* significantly improved the effective control of avocado white root rot on infected plants in comparison with treatments with the fungicide or the antagonist alone. Our study also found that the combination of AgNPs-C with TK could reduce the incidence of MFW and improve the growth of muskmelon, which were in agreement with the aforementioned studies. Moreover, *Trichoderma* sp. and AgNPs both can promote plant growth and development.<sup>58,59</sup> Some *Trichoderma* strains can colonize and interact with roots to improve the uptake of nutrients and secrete bioactive compounds that will be beneficial for increasing plant growth, resistance to disease, and tolerance to abiotic stresses.<sup>58,60</sup> Biosynthesized AgNPs have a beneficial impact on plant growth parameters, such as seed germination, number of leaves, root length and area, shoot length, and fresh weight.<sup>59,61</sup> AgNPs are now known to be an efficient material to enhance phytohormones to a greater extent, which can promote plant growth and improve development.<sup>62</sup> Biosynthesized AgNPs are less toxic in comparison with the chemically synthesized AgNPs.<sup>63</sup> Cui *et al.*<sup>38</sup> used the model insect silkworm (*Bombyx mori*) to evaluate the biosafety of the biosynthesized AgNPs, and found that 50 mg L<sup>-1</sup> of biosynthesized AgNPs had no toxic effect on the silkworm. In this way, based on the previous studies, our results further indicated that the integrated application of AgNPs and *Trichoderma* combinations should be recommended to avoid the development of fungicide resistance by the pathogen, improving the control of MFW and reducing the use of chemical fungicides.

## 5. Conclusions

The combination of fungicide and biocontrol agent (*Trichoderma* sp.) can be used to reduce the fungicide and control MFW in muskmelon production, which provides an alternative approach to realize eco-friendly control of the soilborne diseases. The present study showed that TK had the ability to inhibit the growth and sporulation of FOM and to resist different AgNPs, which had a strong ability to suppress FOM. The AgNPs with high antifungal activity showed the spherical shape of cubic crystal nanoparticles with sizes ranging from 16.5 to 19 nm, and the presence of many functional group moieties to change the properties of AgNPs. The combination application of AgNPs and TK could control the MFW disease, and improve the growth and development of muskmelon. However, the control effect of the combination of AgNPs and TK on MFW in field experiments needs to be further verified. The dosage and method of application also need to be further explored.

## Data availability

All relevant data are within the paper.

## Author contributions

Tong Li: writing – original draft, methodology, formal analysis. Ran Tao: writing – original draft, data curation. Zhen Zhong: conceptualization, methodology, writing – original draft. Xian Liu: supervision, writing – review & editing. Zenggui Gao: writing – review & editing, funding acquisition.

## Conflicts of interest

The authors declare that the research was conducted in the absence of any commercial or financial relationships that could be construed as a potential conflict of interest.

## Acknowledgements

This research was financially supported by the Independent Innovation Fund for Agricultural Science and Technology of Ningxia Hui Autonomous Region [Grant number: NGSB-2021-10-01].

## References

- 1 Z. Zhang, S. Tang, X. Liu, X. Ren, S. Wang and Z. Gao, The Effects of *Trichoderma viride* T23 on Rhizosphere Soil Microbial Communities and the Metabolomics of Muskmelon under Continuous Cropping, *Agronomy*, 2023, **13**, 1092, DOI: [10.3390/agronomy13041092](https://doi.org/10.3390/agronomy13041092).
- 2 Y. Zhou, H. Qiao, H. Gao and S. Li, Effect of Melon Continuous Cropping on Rhizosphere Soil Microorganisms and Enzyme Activities, *Beifang Yuanyu*, 2015, **19**, 158–161, (In Chinese).
- 3 S. Wang, Y. Gao, R. Yang, Z. Zhang, X. Cai, B. Liu, Z. Gao, X. Liu and Y. Yao, Screening and using allelopathic crops to increase the yield of muskmelon (*Cucumis melon* L.), *Allelopathy J.*, 2017, **40**, 117–131.
- 4 J. Blaya, E. Lloret, M. Ros and J. A. Pascual, Identification of predictor parameters to determine agro-industrial compost suppressiveness against *Fusarium oxysporum* and *Phytophthora capsica* diseases in muskmelon and pepper seedlings, *J. Sci. Food Agric.*, 2014, **95**(7), 1482–1490, DOI: [10.1002/jsfa.6847](https://doi.org/10.1002/jsfa.6847).
- 5 Q. Zhao, W. Ran, H. Wang, X. Li, Q. Shen, S. Shen and Y. Xu, Biocontrol of *Fusarium* wilt disease in muskmelon with *Bacillus subtilis* Y-IVI, *BioControl*, 2013, **58**(2), 283–292.
- 6 F. Suárez-Estrella, C. Vargas-García, C. M. J. Lopez and J. M. Capel, Antagonistic activity of bacteria and fungi from horticultural compost against *Fusarium oxysporum* f. sp. melonis, *Crop Prot.*, 2007, **26**, 46–53.
- 7 A. Martínez-Medina, A. Roldán and J. A. Pascual, Interaction between arbuscular mycorrhizal fungi and *Trichoderma harzianum* under conventional and low input fertilization field condition in melon crops: Growth response and *Fusarium* wilt biocontrol, *Appl. Soil Ecol.*, 2011, **47**, 98–105.
- 8 A. A. T. Gava and J. M. Pinto, Biocontrol of melon wilt caused by *Fusarium oxysporum* schlect f. sp. melonis using seed treatment with *Trichoderma* spp. and liquid compost, *Biol. Control*, 2016, **97**, 13–20.



- 9 M. Oskiera, M. Szczech, A. Stębowska, U. Smolińska and G. Bartoszewski, Monitoring of *Trichoderma* species in agricultural soil in response to application of biopreparations, *Biol. Control*, 2011, **113**, 65–72.
- 10 M. Mazzola and S. Freilich, Prospects for biological soilborne disease control: application of indigenous versus synthetic microbiomes, *Phytopathology*, 2017, **107**, 256–263, DOI: [10.1094/PHYTO-09-16-0330-RVW](https://doi.org/10.1094/PHYTO-09-16-0330-RVW).
- 11 A. Zehra, M. Meena, M. K. Dubey, M. Aamir and R. S. Upadhyay, Synergistic effects of plant defense elicitors and *Trichoderma harzianum* on enhanced induction of antioxidant defense system in tomato against fusarium wilt disease, *Bot. Stud.*, 2017, **58**(1), 44, DOI: [10.1186/s40529-017-0198-2](https://doi.org/10.1186/s40529-017-0198-2).
- 12 R. Solis-Palacios, G. Hernández-Ramírez, J. Salinas-Ruiz, J. V. Hidalgo-Contreras and F. C. Gómez-Merino, Effect and compatibility of phosphite with *Trichoderma* sp. isolates in the control of the *Fusarium* species complex causing Pokkah boeng in sugarcane, *Agronomy*, 2021, **11**, 1099, DOI: [10.3390/agronomy11061099](https://doi.org/10.3390/agronomy11061099).
- 13 Q. Ma, Y. Cong, L. Feng, C. Liu, W. Yang, Y. Xin and K. Chen, Effects of mixed culture fermentation of *Bacillus amyloliquefaciens* and *Trichoderma longibrachiatum* on its constituent strains and the biocontrol of tomato *Fusarium* wilt, *J. Appl. Microbiol.*, 2022, **132**, 532–546, DOI: [10.1111/jam.15208](https://doi.org/10.1111/jam.15208).
- 14 Y. Li, S. Jiang, J. Jiang, C. Gao, X. Qi, L. Zhang, S. Sun, Y. Dai and X. Fan, Synchronized efficacy and mechanism of alkaline fertilizer and biocontrol fungi for *Fusarium oxysporum* f. sp. *cubense* tropical race 4, *J. Fungi*, 2022, **8**, 261, DOI: [10.3390/jof8030261](https://doi.org/10.3390/jof8030261).
- 15 X. Zhang, F. Liu, S. Jiang and C. Luo, Inhibition of *Trichoderma* on Some *Fusarium* Pathogens, *Zhongguo Guo-Cai*, 2010, **1**, 11–13, (In Chinese).
- 16 S. Wang, J. Ma, X. Wang, Y. Li and J. Chen, Combined application of *Trichoderma harzianum* SH2303 and difenoconazole-propiconazolein controlling Southern corn leaf blight disease caused by *Cochliobolus heterostrophus* in maize, *J. Integr. Agric.*, 2019, **18**(9), 2063–2071.
- 17 A. Jamil and S. Ashraf, Integrated approach for managing *Fusarium* wilt of chickpea using *Azadirachta indica* leaf extract, *Trichoderma harzianum* and Bavistin, *Fitopatol. Bras.*, 2022, **47**, 727–736, DOI: [10.1007/s40858-022-00533-w](https://doi.org/10.1007/s40858-022-00533-w).
- 18 C. Zhang, W. Wang, M. Xue, Z. Liu, Q. Zhang, J. Hou, M. Xing, R. Wang and T. Liu, The Combination of a Biocontrol Agent *Trichoderma asperellum* SC012 and Hymexazol Reduces the Effective Fungicide Dose to Control *Fusarium* Wilt in Cowpea, *J. Fungi*, 2021, **7**, 685, DOI: [10.3390/jof7090685](https://doi.org/10.3390/jof7090685).
- 19 M. F. Gonzalez, F. Magdama, L. Galarza, D. Sosa and C. Romero, Evaluation of the sensitivity and synergistic effect of *Trichoderma reesei* and mancozeb to inhibit under in vitro conditions the growth of *Fusarium oxysporum*, *Commun. Integr. Biol.*, 2020, **13**(1), 160–169, DOI: [10.1080/19420889.2020.1829267](https://doi.org/10.1080/19420889.2020.1829267).
- 20 S. C. Dubey, V. Singh, K. Priyanka, B. K. Upadhyay and B. Singh, Combined application of fungal and bacterial bioagents, together with fungicide and *Mesorhizobium* for integrated management of *Fusarium* wilt of chickpea, *BioControl*, 2015, **60**, 413–424, DOI: [10.1007/s10526-015-9653-8](https://doi.org/10.1007/s10526-015-9653-8).
- 21 T. L. Widmer, Compatibility of *Trichoderma asperellum* isolates to selected soil fungicides, *Crop Prot.*, 2019, **120**, 91–96, DOI: [10.1016/j.cropro.2019.02.017](https://doi.org/10.1016/j.cropro.2019.02.017).
- 22 B. Sánchez-Montesinos, M. Santos, A. Moreno-Gavira, T. Marín-Rodulfo, F. J. Gea and F. Diáñez, Biological control of fungal diseases by *Trichoderma aggressivum* f. *europaeum* and its compatibility with fungicides, *J. Fungi*, 2021, **7**, 598, DOI: [10.3390/jof7080598](https://doi.org/10.3390/jof7080598).
- 23 Q. H. Tran, V. Q. Nguyen and A. T. Le, Silver nanoparticles: synthesis, properties, toxicology, applications and perspectives, *Adv. Nat. Sci.:Nanosci. Nanotechnol.*, 2013, **4**, 033001, DOI: [10.1088/2043-6262/4/3/033001](https://doi.org/10.1088/2043-6262/4/3/033001).
- 24 K. A. Altammar, A review on nanoparticles: characteristics, synthesis, applications, and challenges, *Front. Microbiol.*, 2023, **14**, 1155622, DOI: [10.3389/fmicb.2023.1155622](https://doi.org/10.3389/fmicb.2023.1155622).
- 25 Y. Jian, X. Chen, T. Ahmed, Q. Shang, S. Zhang, Z. Ma and Y. Yin, Toxicity and action mechanisms of silver nanoparticles against the mycotoxin-producing fungus *Fusarium graminearum*, *J. Adv. Res.*, 2022, **38**, 1–12, DOI: [10.1016/j.jare.2021.09.006](https://doi.org/10.1016/j.jare.2021.09.006).
- 26 M. A. El-Naggar, A. M. Alrajhi, M. M. Fouda, E. M. Abdelkareem, T. M. Thabit and N. A. Bouqellah, Effect of silver nanoparticles on toxigenic *Fusarium* spp. and deoxynivalenol secretion in some grains, *J. AOAC Int.*, 2018, **101**, 1534–1541, DOI: [10.5740/jaoacint.17-0442](https://doi.org/10.5740/jaoacint.17-0442).
- 27 B. Xue, D. He, S. Gao, D. Wang, K. Yokoyama and L. Wang, Biosynthesis of silver nanoparticles by the fungus *Arthroderma fulvum* and its antifungal activity against genera of *Candida*, *Aspergillus* and *Fusarium*, *Int. J. Nanomed.*, 2016, **11**, 1899–1906, DOI: [10.2147/IJN.S98339](https://doi.org/10.2147/IJN.S98339).
- 28 A. Kędziora, M. Speruda, E. Krzyżewska, J. Rybka, A. Łukowiak and G. Bugła-Płoskońska, Similarities and differences between silver ions and silver in nanoforms as antibacterial agents, *Int. J. Mol. Sci.*, 2018, **19**(2), 444, DOI: [10.3390/ijms19020444](https://doi.org/10.3390/ijms19020444).
- 29 S. Wahab, T. Khan, M. Adil and A. Khan, Mechanistic aspects of plant-based silver nanoparticles against multi-drug resistant bacteria, *Heliyon*, 2021, **7**, e07448, DOI: [10.1016/j.heliyon.2021.e07448](https://doi.org/10.1016/j.heliyon.2021.e07448).
- 30 H. Shi, H. Wen, S. Xie, Y. Li, Y. Chen, Z. Liu, N. Jiang, J. Qiu, X. Zhu, F. Lin and Y. Kou, Antifungal activity and mechanisms of AgNPs and their combination with azoxystrobin against *Magnaporthe oryzae*, *Environ. Sci.:Nano*, 2023, **10**, 2412, DOI: [10.1039/d3en00168g](https://doi.org/10.1039/d3en00168g).
- 31 X. Liu, T. Li, X. Cui, R. Tao and Z. Gao, Antifungal mechanism of nanosilver biosynthesized with *Trichoderma longibrachiatum* and its potential to control muskmelon *Fusarium* wilt, *Sci. Rep.*, 2024, **14**(1), 20242, DOI: [10.1038/s41598-024-71282-w](https://doi.org/10.1038/s41598-024-71282-w).
- 32 A. J. Huh and Y. J. Kwon, “Nanoantibiotics”: a new paradigm for treating infectious diseases using nanomaterials in the antibiotics resistant era, *J. Controlled Release*, 2011, **156**, 128–145.



- 33 R. Benoit, K. J. Wilkinson and S. Sauve, Partitioning of silver and chemical speciation of free Ag in soils amended with nanoparticles, *Chem. Cent. J.*, 2013, **7**, 75, DOI: [10.1186/1752-153X-7-75](#).
- 34 W. Chunjaturas, J. A. Ferguson, W. Rattanapichai, M. J. Sadowsky and K. Sajjaphan, Shift of bacterial community structure in two Thai soil series affected by silver nanoparticles using ARISA, *World J. Microbiol. Biotechnol.*, 2014, **30**, 2119–2124, DOI: [10.1007/s11274-014-1633-0](#).
- 35 V. Shah, D. Collins, V. K. Walker and S. Shah, The impact of engineered cobalt, iron, nickel and silver nanoparticles on soil bacterial diversity under field conditions, *Environ. Res. Lett.*, 2014, **9**, 024001, DOI: [10.1088/1748-9326/9/2/024001](#).
- 36 S. Mishra and H. Singh, Biosynthesized silver nanoparticles as a nanoweapon against phytopathogens: exploring their scope and potential in agriculture, *Appl. Microbiol. Biotechnol.*, 2015, **99**(3), 1097–1107, DOI: [10.1007/s00253-014-6296-0](#).
- 37 S. Zhang, B. Zhao, X. Liu, J. Li, Z. Gao and X. Huang, DNA sequencing and UP-PCR characterization of *Fusarium oxysporum* isolates from three Cucurbit species, *Plant Pathol. J.*, 2013, **12**(2), 78–84, DOI: [10.3923/ppj.2013.78.84](#).
- 38 X. Cui, Z. Zhong, R. Xia, X. Liu and L. Qin, Biosynthesis optimization of silver nanoparticles (AgNPs) using *Trichoderma longibrachiatum* and biosafety assessment with silkworm (*Bombyx mori*), *Arabian J. Chem.*, 2022, **15**(10), 104142, DOI: [10.1016/j.arabjc.2022.104142](#).
- 39 W. A. Lotfy, B. M. Alkersh, S. A. Sabry and H. A. Ghazlan, Biosynthesis of silver Nanoparticles by *Aspergillus terreus*: characterization, optimization, and biological Activities, *Front. Bioeng. Biotechnol.*, 2021, **9**, 633468, DOI: [10.3389/fbioe.2021.633468](#).
- 40 H. Chhipa, Nanofertilizers and nanopesticides for agriculture, *Environ. Chem. Lett.*, 2017, **15**, 15–22, DOI: [10.1007/s10311-016-0600-4](#).
- 41 J. Li, K. Rong, H. Zhao, F. Li, Z. Lu and R. Chen, Highly selective antibacterial activities of silver nanoparticles against *Bacillus subtilis*, *J. Nanosci. Nanotechnol.*, 2013, **13**, 6806–6813, DOI: [10.1166/jnn.2013.7781](#).
- 42 M. Qu, W. Yao, X. Cui, R. Xia, L. Qin and X. Liu, Biosynthesis of silver nanoparticles (AgNPs) employing *Trichoderma* strains to control empty-gut disease of oak silkworm (*Antheraea pernyi*), *Mater. Today Commun.*, 2021, **28**, 102619, DOI: [10.1016/j.mtcomm.2021.102619](#).
- 43 M. Saravanan, S. K. Barik, D. MubarakAli, P. Prakash and A. Pugazhendhi, Synthesis of silver nanoparticles from *Bacillus brevis* (NCIM 2533) and their antibacterial activity against pathogenic bacteria, *Microb. Pathog.*, 2018, **116**, 221–226.
- 44 H. Wen, H. Shi, N. Jiang, J. Qiu, F. Lin and Y. Kou, Antifungal mechanisms of silver nanoparticles on mycotoxin producing rice false smut fungus, *iScience*, 2023, **26**, 105763, DOI: [10.1016/j.isci.2022.105763](#).
- 45 S. Das, L. Langbang, M. Haque, V. K. Belwal, K. Aguan and A. S. Roy, Biocompatible silver nanoparticles: An investigation into their protein binding efficacies, antibacterial effects and cell cytotoxicity studies, *J. Pharm. Anal.*, 2021, **1**, 422–434, DOI: [10.1016/j.jpha.2020.12.003](#).
- 46 A. L. M. Terra, R. D. C. Kosinski, J. B. Moreira, J. A. V. Costa and M. G. Morais, Microalgae biosynthesis of silver nanoparticles for application in the control of agricultural pathogens, *J. Environ. Sci. Health, Part B*, 2019, **54**(8), 709–716.
- 47 J. J. Castellano, S. M. Shafii, F. Ko, G. Donate, T. E. Wright, R. J. Mannari, W. G. Payne, D. J. Smith and M. C. Robson, Comparative evaluation of silver-containing antimicrobial dressings and drugs, *Int. Wound J.*, 2007, **4**(2), 114–122, DOI: [10.1111/j.1742-481X.2007.00316.x](#).
- 48 Y. K. Jo, B. H. Kim and G. Jung, Antigungal activity of silver ions and nanoparticles on phytopathogenic fungi, *Plant Dis.*, 2009, **93**, 1037–1043, DOI: [10.1094/PDIS-93-10-1037](#).
- 49 S. A. Shahriar, M. N. Islam, C. N. W. Chun, P. Kaur, M. A. Rahim, M. M. Islam, J. Uddain and S. Siddiquee, Microbial metabolomics interaction and ecological challenges of *Trichoderma* species as biocontrol inoculant in crop rhizosphere, *Agronomy*, 2022, **12**, 900, DOI: [10.3390/agronomy12040900](#).
- 50 R. Tyśkiewicz, A. Nowak, E. Ozimek and J. Jaroszuk-Scisiel, *Trichoderma*: The current status of its application in agriculture for the biocontrol of fungal phytopathogens and stimulation of plant growth, *Int. J. Mol. Sci.*, 2022, **23**, 2329, DOI: [10.3390/ijms23042329](#).
- 51 X. Yao, H. Guo, K. Zhang, M. Zhao, J. Ruan and J. Chen, *Trichoderma* and its role in biological control of plant fungal and nematode disease, *Front. Microbiol.*, 2023, **14**, 1160551, DOI: [10.3389/fmicb.2023.1160551](#).
- 52 S. Halifu, X. Deng, X. Song, R. Song and X. Liang, Inhibitory mechanism of *Trichoderma virens* ZT05 on *Rhizoctonia solani*, *Plants*, 2020, **9**, 912, DOI: [10.3390/plants9070912](#).
- 53 F. A. Mohiddin, S. A. Padder, A. H. Bhat, M. A. Ahanger, A. B. Shikari and S. H. Wani, *et al.*, Phylogeny and optimization of *Trichoderma harzianum* for Chitinase production: evaluation of their antifungal behaviour against the prominent soil borne Phyto-pathogens of temperate India, *Microorganisms*, 2021, **9**(9), 1962, DOI: [10.3390/microorganisms9091962](#).
- 54 H. Xu, L. Yan, M. Zhang, X. Chang, D. Zhu and D. Wei, *et al.*, Changes in the density and composition of rhizosphere pathogenic *Fusarium* and beneficial *Trichoderma* contributing to reduced root rot of intercropped soybean, *Pathogens*, 2022, **11**, 478, DOI: [10.3390/pathogens11040478](#).
- 55 R. Lahlali, S. Ezrari, N. Radouane, J. Kenfaoui, Q. Esmaeel, H. El Hamss, Z. Belabess and E. A. Barka, Biological control of plant pathogens: a global perspective, *Microorganisms*, 2022, **10**, 596, DOI: [10.3390/microorganisms10030596](#).
- 56 M. Jangir, S. Sharma and S. Sharma, Synergistic effect of oilseed cake and biocontrol agent in the suppression of *Fusarium wilt* in *Solanum lycopersicum*, *Braz. J. Microbiol.*, 2020, **51**, 1929–1939, DOI: [10.1007/s42770-020-00344-8](#).
- 57 D. Ruano-Rosa, I. Arjona-Girona and C. J. Lopez-Herrera, Integrated control of avocado white root rot combining low concentrations of fluazinam and *Trichoderma* spp, *Crop Prot.*, 2018, **112**, 363–370, DOI: [10.1016/j.cropro.2017.06.024](#).
- 58 R. Hermosa, A. Viterbo, I. Chet and E. Monte, Plant-beneficial effects of *Trichoderma* and of its genes, *Microbiology*, 2012, **158**, 17–25, DOI: [10.1099/mic.0.052274-0](#).



- 59 B. Jasim, R. Thomas, J. Mathew and E. K. Radhakrishnan, Plant growth and diosgenin enhancement effect of silver nanoparticles in Fenugreek (*Trigonella foenum-graecum* L.), *Saudi Pharm. J.*, 2017, **25**(3), 443–447, DOI: [10.1016/j.jsps.2016.09.012](https://doi.org/10.1016/j.jsps.2016.09.012).
- 60 S. L. Woo, M. Ruocco, F. Vinale, M. Nigro, R. Marra, N. Lombardi, A. Pascale, S. Lanzuise, G. Manganiello and M. Lorito, Trichoderma-based products and their widespread use in agriculture, *Open Mycol. J.*, 2014, **8**(Suppl-1, M4), 71–126.
- 61 N. Khan and A. Bano, Role of plant growth promoting Rhizobacteria and Ag-nano particle in the bioremediation of heavy metals and maize growth under municipal wastewater irrigation, *Int. J. Phytorem.*, 2015, **18**(3), 211–221, DOI: [10.1080/15226514.2015.1064352](https://doi.org/10.1080/15226514.2015.1064352).
- 62 A. R. Nayana, B. J. Joseph, A. Jose and E. K. Radhakrishnan, Nanotechnological advances with PGPR applications, in *Sustainable Agriculture Reviews, 41-Nanotechnology for plant growth and development*, Springer Nature Switzerland AG, Switzerland, 2020, pp. 201–214.
- 63 D. Sharma, S. Kanchi and K. Bisetty, Biogenic synthesis of nanoparticles: a review, *Arabian J. Chem.*, 2019, **12**, 3576–3600, DOI: [10.1016/j.arabjc.2015.11.002](https://doi.org/10.1016/j.arabjc.2015.11.002).

